Arnold Engineering Development Center, Wright-Patterson AFB, Ohio.

[4]Gates, D. G., "Measurements of Upstream History Effects in Compressible Turbulent Boundary Layers," NOLTR 73-152, July 1973, Naval Ordnance Laboratory, Silver Spring, Md.

Target Intensity Enhancement for Repetitively Pulsed Laser Beams

J. Q. Lilly* and T. G. Miller†
U. S. Army Missile Research, Development, and Engineering Lab., U. S. Army Missile Command, Redstone Arsenal, Ala.

Introduction

A POSSIBLE method of minimizing the thermal blooming associated with the propagation of laser radiation through the atmosphere is to use repetitively pulsed lasers. This approach allows maintenance of high average power on target and, by optimizing the pulse width and intervals between pulses, permit convective clearing of the heated air between pulses. Results presented by Wallace and Lilly[1] showed that peak time-averaged intensities could be four or more times as great at low pulse repetition frequency (PRF) as continuous wave (CW) propagation at the same average power. At higher PRF, the peak intensities produced approach CW conditions and essentially no advantage is obtained. However, the results presented did not consider the effects of varying beam power or focal length.

In this paper, the dependence of peak intensity on target on the laser power level is theoretically investigated at low PRF for both focused and collimated beams. For the collimated case, the enhancement, or increase in peak intensity above the diffraction-limited (unbloomed) intensity, a result recently confirmed by experiment,[2] is investigated further. The results of Gebhardt et al.[2] showed that the peak intensity obtained for subsequent pulses could exceed the first pulse peak intensity by 20% or more. In this paper results are presented showing that this enhancement could reach 75% for optimum power beams.

Summary of Theory

The basic governing equations for thermal blooming of laser beams are the fluid dynamics conservation equations for determining atmospheric variables and the electromagnetic wave equations governing the laser energy distribution. To couple the solutions of these two basic equations, an additional equation relating the index of refraction and the air density is required.

For a repetitively pulsed laser beam consisting of a series of pulses of duration t_p separated by duration t_s where $t_p \ll t_s$, the solution for the density variation in the beam for the Nth pulse becomes

$$\left(\frac{\rho-\rho_\infty}{\rho_\infty}\right)^N = -\left(\frac{\gamma-1}{\gamma}\right)\frac{\alpha I_0 t_p}{p_\infty} \sum_{i=0}^{N-1} I_i\left[x-\frac{U_\infty t_s}{R_m}(N-i), y, z\right] \tag{1}$$

where

I_i = the intensity distribution of the ith pulse
ρ_∞ = the atmospheric ambient density
γ = the specific heat ratio
α = the absorption coefficient
I_0 = the beam peak intensity at $z=0$
p_∞ = the atmospheric pressure
x,y = the coordinates in the plane of the beam normalized with respect to R_m, the initial beam radius
z = the coordinate along the beam
U_∞ = the wind velocity transverse to the beam

The wind component can be modified to account for beam slewing, stagnation zones, etc. Additional terms accounting for pressure relaxation effects and single pulse blooming during time t_p have been neglected. Kinetic effects and bleaching are considered unimportant in the present analysis. The single term retained accounts for the overlapping effects of each succeeding pulse being transmitted through the air heated by the previous pulses. The shift, which produces overlapping between pulses is due to wind effects and is represented by $U_\infty t_s/R_m$. Defining one flow time as the time required for the wind to sweep across the beam at the aperture ($z=0$), the number of overlapping pulses contained within the beam is $2R_m/U_\infty t_s$. This quantity is defined as the pulses per flow time (PPFT) and specifies the number of previous pulses affecting the transmission of any given pulse. After leaving the aperture, the number of overlapping pulses changes as the beam focuses or defocuses and a change in wind velocity such as beam slewing or stagnation will similarly alter the overlapping effect.

For laser propagation in the atmosphere, the appropriate form of Maxwell's electromagnetic wave equation is the paraxial approximation represented for the Nth pulse by

$$2iF\frac{\partial A^N}{\partial z} + \nabla^2 A^N + \frac{2F^2 z_f^2 (n_\infty - 1)}{R_m^2} \times \left(\frac{\rho-\rho_\infty}{\rho_\infty}\right)^N A^N = 0 \tag{2}$$

where

F = the Fresnel number $2\pi R_m^2/\lambda z_f$
A = the complex amplitude
z_f = the range to the focus
n_∞ = the ambient index of refraction

The amplitude distribution at the aperture is required as a boundary condition and an additional equation relating index of refraction to density is simply a linear expression.

Whereas the basic governing equations presented can be solved entirely by finite-difference methods, the requirements in computation time and computer storage are enormous. A particularly straightforward and efficient method of solution is to use Fourier transforms utilizing the Fast-Fourier Transform (FFT) algorithm.[3] This method is typically many times faster than ordinary finite differences and usually requires less computer storage. Because the air density is explicitly determined once the intensity distribution is known, it remains to solve the wave equation for the amplitude distribution then I is calculated from $I=AA^*$. The wave equation is solved by introducing a phase-front distortion term proportional to the density changes produced by heating, finite differencing in the propagation (z) direction, and taking the Fourier transform of the result thus giving

$$\overline{A^N_{k+1}} = \overline{A_k^N \exp(i\Delta\varphi)_k^N} \exp\left[\frac{-i\Delta z(p^2+q^2)}{2F}\right] \tag{3}$$

The barred quantities indicate FFT transformed values, φ is the distortion parameter; p and q are the transform variables

Presented as Paper 75-718 at the AIAA 10th Thermophysics Conference, Denver, Colo., May 27-29, 1975; submitted Aug. 4, 1976; revision received Oct. 29, 1976.

Index categories: Hydrodynamics; Lasers.

*Aerospace Engineer, Physical Sciences Directorate.

†Research Physicist, High Energy Laser Directorate.

that must be chosen at discrete intervals in the transformed plane according to the relations

$$M(\Delta x)(\Delta p) = L(\Delta y)(\Delta q) = 2\pi \tag{4}$$

where M and L are the number of mesh points in the respective directions. The subscript k represents the z position of the computation along the propagation direction so that the quantity $\overline{A^N_{k+1}}$ is the solution for the amplitude at the next z station for the Nth pulse after the inverse transform of the $\overline{A^N_{k+1}}$ array is completed using the FFT routine. Computation in the z direction typically requires 10 steps compared to perhaps 100 steps for a finite-difference solution. The time required to make a complete coupled computation for each pulse transmitted using 10 z steps with a 64×64 array in the x-y plane is approximately 20 sec using a computer such as the CDC 6600. As was illustrated by Wallace and Lilly,[1] steady-state density distribution is attained after one flow time; hence, the number of pulses that must by transmitted to reach steady intensity distribution is one more than the PPFT.

A parametric investigation of laser propagation through the atmosphere has resulted in the development of a scaling-law computation for peak target intensities of repetitively pulsed and CW laser beams.[4] Functionally, the intensity on target can be represented in terms of the nondimensional governing parameters as

$$I/I_{DL} = \Phi(N_F, N_\alpha, N_P, N_D) \tag{5}$$

where I_{DL} is the diffraction limited intensity and the parameters are

$N_F = 2\pi R_m^2/\lambda z_f$, the Fresnel number
$N_\alpha = \alpha z_f$, the extinction number
$N_P = 2R_m/U_\infty t_s$, pulse number or PPFT

$$N_D = \frac{2\pi z_f}{\lambda}(n_\infty - 1)\left(\frac{\gamma - 1}{\gamma}\right)\frac{\alpha I_0 R_m}{P_\infty U_\infty}, \text{distortion number.}$$

These four dimensionless parameters represent the effects of focusing, absorption, pulse rate, and power, respectively. An additional number representing beam-slewing effects has been omitted in this analysis. The results of this investigation will be presented in terms of these parameters in the following section.

Results

The results presented in this section were obtained to investigate the dependence of peak target intensity on the laser power level at low pulse number for focused beams at a constant Fresnel number and for collimated beams at the same range z as for the focused beams. Investigation of peak pulse intensity enhancement for a collimated beam was of special interest because the experiment of Gebhardt et al. at United Aircraft Research Laboratories had confirmed predictions that a collimated beam would be focused by the effects of heating from previous pulses at low PRF.[2]

Conditions chosen for the computations were for an infinite, circular, Gaussian beam, R_m was the initial beam radius to the $1/e^2$ intensity level, αz_f was held fixed at 0.8, Fresnel number at 5.93 for the focused beam, and the pulse number was held constant at 2 PPFT. To illustrate the improvement in pulsed propagation at low pulse number, the results for focused beams will be shown compared with CW beams at the same average power level, Fresnel number, extinction number, and distortion number. Constant intensity contour plots chosen to illustrate the relative spot sizes show intensity levels at 90%, 70%, 50%, 30%, and 13.5% of the peak intensity of that spot.

Figure 1 presents calculated peak intensities obtained at the focal plane for a focused beam. Shown here as a function of the distortion number for 2 PPFT and CW at the same

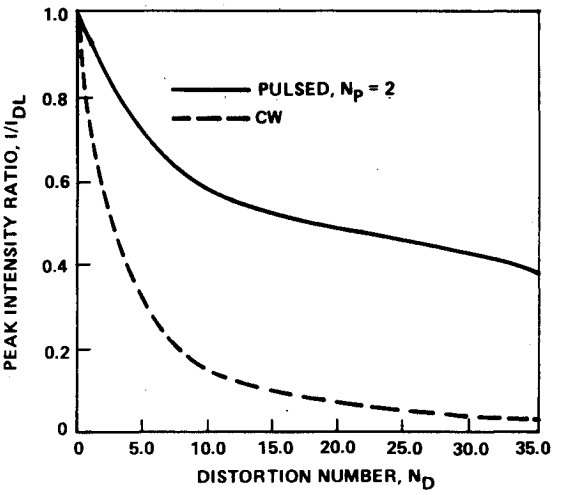

Fig. 1 Peak intensity ratio for focused beams, $N_F = 5.93$, $N_\alpha = 0.8$.

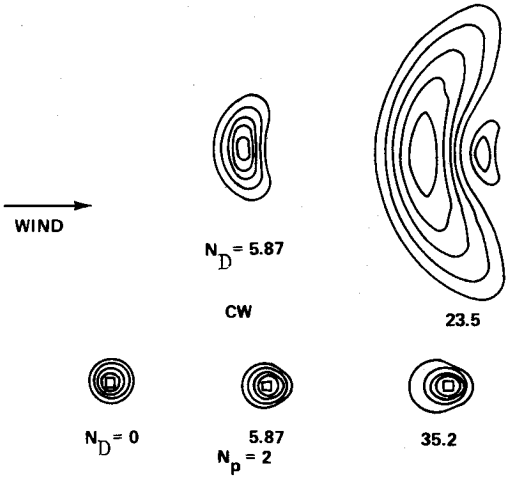

Fig. 2 Constant intensity contours for focused beams, $N_F = 5.93$, $N_\alpha = 0.8$.

average power, these curves illustrate the drop in peak intensity to less than 5% of diffraction limited for CW beams compared to approximately 40% for the pulsed beam. Spot size as shown on the contour plots in Fig. 2 remains small for pulsed beams in comparison to CW beams transmitting the same total power. It is noted that the spot shape for pulsed propagation at low pulse number is of basically different character than for CW beams. This is attributed to the beam being transmitted over much of the latter part of its path is undisturbed air because the decreasing beam size overlaps less and less of the heated air from previous pulses; hence, its shape more closely resembles the unbloomed spot.

Results for the collimated beam calculations are presented in Figs. 3 and 4. Figure 3 presents the ratio of peak intensity obtained for the second pulse after the initial unbloomed pulse to the peak intensity of the initial pulse. Shown as a function of N_D for the same extinction term, N_α as the focused beams, this curve shows that the enhancement ratio increases to a peak value of almost 1.8 and decreases thereafter as beam power is increased. The contour plots of Fig. 4 show that the peak intensity enhancement grows with increasing flatness of the spot in the downwind (right) direction, but eventually decreases as the growth in spot size in the lateral direction becomes predominant. Examined from a different viewpoint, it is seen that rays in the overlapping part of the beam are focused by the negative slope in index of refraction produced by heating from the previous pulse resulting in increased intensity in the upwind (unheated) part of the beam.

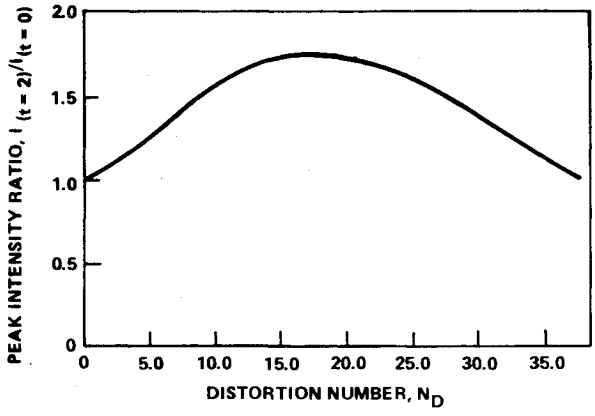

Fig. 3 Peak intensity ratio of second pulse to initial pulse for collimated beams, $N_P = 2$.

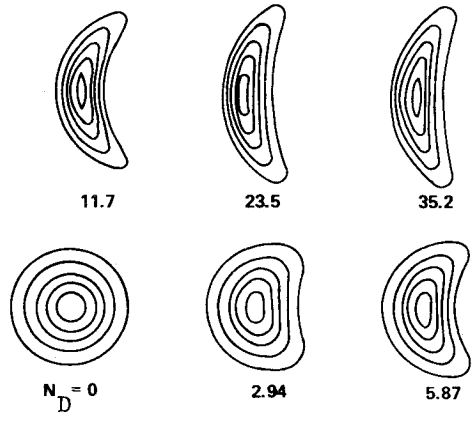

Fig. 4 Constant intensity contours for collimated beams, $N_P = 2$.

Conclusions

Presented here are results that demonstrate the improvement in peak intensity obtained by propagation of low-pulse-rate beams compared to CW beams of the same average transmitted power. These results have been obtained without consideration for such practical limitations as atmospheric breakdown, which could be encountered with low-pulse-rate, high-average-power pulsed lasers. These results are subject to the stated conditions of negligible pressure relaxation, negligible single pulse blooming effects, and the assumed Gaussian beam profile. However, it should be pointed out that the method of solution presented is not limted to these restrictive conditions, but may be employed for analyzing lasers with non-Gaussian beam profiles, beams from oscillators with central obscuration, or nonsymmetric beam profiles. The basic method of solution used here has now been extended by other investigators to analyze the effects of atmospheric turbulence, transonic slewing beams, beams with stagnation zones, and beams from lasers with compensating optical output to further reduce thermal-blooming effects.

Acknowledgment

We gratefully acknowledge the helpful suggestions made by Dr. James Wallace of Far Field, Inc. in the course of this investigation.

References

[1]Wallace, J. and Lilly, J. Q., "Thermal Blooming of Repetitively Pulsed Laser Beams," *Journal of the Optical Society of America*, Vol. 64, Dec. 1974, pp. 1651-1655.

[2]Gebhardt, F. G., Berger, P. J., Smith, D. C., Burdick, B., and Tripodi, R., "Reduction of Thermal Blooming by Beam Optimization," United Aircraft Research Lab., East Hartford, Conn., Rept. N921769-4, Oct. 1974.

[3]Cooley, J. W., Lewis, P. A. W., and Welch, P. D., "The Finite Fourier Transform," *IEEE Transactions on Audio and Electroacoustics*, Vol. AU-17, June 1969, pp. 77-85.

[4]Lilly, J. Q., "Simplified Calculation of Laser Beam Propagation Through the Atmosphere," US Army Missile Command, Redstone Arsenal, Ala., Rept. RH-76-8, Jan. 1976.

Total Head/Static Measurements of Skin Friction and Surface Pressure

A. Bertelrud*
FFA, The Aeronautical Research Institute of Sweden, Bromma, Sweden

Introduction

MEASUREMENT of the local friction force is an important objective in many experiments. Yet it seems that no method is both accurate and practical in all applications of potential interest. Various methods have been used,[1] among which the Preston tube[2,3] seems to be one of the most simple and reliable. By measuring the differential between the total head and the local static pressure it is possible to obtain the friction force from a calibration curve. But it is often difficult or costly to measure the static pressure with the required accuracy. This may be the case for instance near the trailing edge of a wing model, and generally on models not originally intended for static pressure investigations. It is also difficult to establish where a static pressure tap should be located to be undisturbed by the presence of the Preston tube. Different remedies to this problem have been suggested; among others Gupta[4] suggested the use of a double Preston tube of different outer diameters and with one tube cut at 45°.

In the present report, another approach is suggested. In view of all the difficulties encountered in obtaining the correct static pressure and the necessity of drilling holes in the surface (or placing a static pressure probe somewhere outside the boundary layer) it appears simpler to measure the static pressure in the center plane of the tube at a specified downstream distance from the leading edge of the tube provided this can be related to the actual static pressure at the tip. This will not be the true static pressure, but the deviations are small and can be accounted for. The probe may be located anywhere within the measurement area like the Gupta probe but will give larger differential pressures than the latter, which is desirable for improved accuracy. One disadvantage of the present method is that small probes are difficult to make.

The use of the new probe is based on knowledge of the flow around surface cylinders aligned with the flow in a nominally constant pressure boundary layer. In Ref. 5 such information has been collected in the form of velocity profiles, pressure distributions, and flow visualizations. It appears that a static pressure tap located at a distance $L/D > 2$ downstream of the leading edge is not much influenced by the local pressure gradient due to the flow field around the cylinder. The pressure tap should preferably be located outside the pressure peak in the vicinity of the leading edge, but should be as near the front as possible to minimize the influence from external longitudinal pressure gradients. As a compromise the probe illustrated in Fig. 1 was made, with dimensions $D = 3$ mm, $L/D = 5$. A limited investigation was undertaken to determine the L/D effects, covering $L/D = 5$ to 2. In the arguments previously presented the wall thickness has been ignored as it

Received Aug. 10, 1976; revision received Dec. 8, 1976.
Index category: Boundary Layers and Convective Heat Transfer – Turbulent.

*Research Engineer. Member AIAA.